Measurements of Branching Fraction, Polarization, and Charge Asymmetry of $B^\pm \to \rho^\pm \rho^0$ and a Search for $B^\pm \to \rho^\pm f_0(980)$

B. Aubert,[1] M. Bona,[1] D. Boutigny,[1] F. Couderc,[1] Y. Karyotakis,[1] J. P. Lees,[1] V. Poireau,[1] V. Tisserand,[1] A. Zghiche,[1]
E. Grauges,[2] A. Palano,[3] J. C. Chen,[4] N. D. Qi,[4] G. Rong,[4] P. Wang,[4] Y. S. Zhu,[4] G. Eigen,[5] I. Ofte,[5] B. Stugu,[5]
G. S. Abrams,[6] M. Battaglia,[6] D. N. Brown,[6] J. Button-Shafer,[6] R. N. Cahn,[6] E. Charles,[6] M. S. Gill,[6] Y. Groysman,[6]
R. G. Jacobsen,[6] J. A. Kadyk,[6] L. T. Kerth,[6] Yu. G. Kolomensky,[6] G. Kukartsev,[6] G. Lynch,[6] L. M. Mir,[6] T. J. Orimoto,[6]
M. Pripstein,[6] N. A. Roe,[6] M. T. Ronan,[6] W. A. Wenzel,[6] P. del Amo Sanchez,[7] M. Barrett,[7] K. E. Ford,[7] T. J. Harrison,[7]
A. J. Hart,[7] C. M. Hawkes,[7] A. T. Watson,[7] T. Held,[8] H. Koch,[8] B. Lewandowski,[8] M. Pelizaeus,[8] K. Peters,[8] T. Schroeder,[8]
M. Steinke,[8] J. T. Boyd,[9] J. P. Burke,[9] W. N. Cottingham,[9] D. Walker,[9] D. J. Asgeirsson,[10] T. Cuhadar-Donszelmann,[10]
B. G. Fulsom,[10] C. Hearty,[10] N. S. Knecht,[10] T. S. Mattison,[10] J. A. McKenna,[10] A. Khan,[11] P. Kyberd,[11] M. Saleem,[11]
D. J. Sherwood,[11] L. Teodorescu,[11] V. E. Blinov,[12] A. D. Bukin,[12] V. P. Druzhinin,[12] V. B. Golubev,[12] A. P. Onuchin,[12]
S. I. Serednyakov,[12] Yu. I. Skovpen,[12] E. P. Solodov,[12] K. Yu Todyshev,[12] M. Bondioli,[13] M. Bruinsma,[13] M. Chao,[13]
S. Curry,[13] I. Eschrich,[13] D. Kirkby,[13] A. J. Lankford,[13] P. Lund,[13] M. Mandelkern,[13] R. K. Mommsen,[13] W. Roethel,[13]
D. P. Stoker,[13] S. Abachi,[14] C. Buchanan,[14] S. D. Foulkes,[15] J. W. Gary,[15] O. Long,[15] B. C. Shen,[15] K. Wang,[15] L. Zhang,[15]
H. K. Hadavand,[16] E. J. Hill,[16] H. P. Paar,[16] S. Rahatlou,[16] V. Sharma,[16] J. W. Berryhill,[17] C. Campagnari,[17] A. Cunha,[17]
B. Dahmes,[17] T. M. Hong,[17] D. Kovalskyi,[17] J. D. Richman,[17] T. W. Beck,[18] A. M. Eisner,[18] C. J. Flacco,[18] C. A. Heusch,[18]
J. Kroseberg,[18] W. S. Lockman,[18] G. Nesom,[18] T. Schalk,[18] B. A. Schumm,[18] A. Seiden,[18] P. Spradlin,[18] D. C. Williams,[18]
M. G. Wilson,[18] J. Albert,[19] E. Chen,[19] A. Dvoretskii,[19] F. Fang,[19] D. G. Hitlin,[19] I. Narsky,[19] T. Piatenko,[19] F. C. Porter,[19]
A. Ryd,[19] G. Mancinelli,[20] B. T. Meadows,[20] K. Mishra,[20] M. D. Sokoloff,[20] F. Blanc,[21] P. C. Bloom,[21] S. Chen,[21]
W. T. Ford,[21] J. F. Hirschauer,[21] A. Kreisel,[21] M. Nagel,[21] U. Nauenberg,[21] A. Olivas,[21] W. O. Ruddick,[21] J. G. Smith,[21]
K. A. Ulmer,[21] S. R. Wagner,[21] J. Zhang,[21] A. Chen,[22] E. A. Eckhart,[22] A. Soffer,[22] W. H. Toki,[22] R. J. Wilson,[22]
F. Winklmeier,[22] Q. Zeng,[22] D. D. Altenburg,[23] E. Feltresi,[23] A. Hauke,[23] H. Jasper,[23] J. Merkel,[23] A. Petzold,[23]
B. Spaan,[23] T. Brandt,[24] V. Klose,[24] H. M. Lacker,[24] W. F. Mader,[24] R. Nogowski,[24] J. Schubert,[24] K. R. Schubert,[24]
R. Schwierz,[24] J. E. Sundermann,[24] A. Volk,[24] D. Bernard,[25] G. R. Bonneaud,[25] E. Latour,[25] Ch. Thiebaux,[25] M. Verderi,[25]
P. J. Clark,[26] W. Gradl,[26] F. Muheim,[26] S. Playfer,[26] A. I. Robertson,[26] Y. Xie,[26] M. Andreotti,[27] D. Bettoni,[27] C. Bozzi,[27]
R. Calabrese,[27] G. Cibinetto,[27] E. Luppi,[27] M. Negrini,[27] A. Petrella,[27] L. Piemontese,[27] E. Prencipe,[27] F. Anulli,[28]
R. Baldini-Ferroli,[28] A. Calcaterra,[28] R. de Sangro,[28] G. Finocchiaro,[28] S. Pacetti,[28] P. Patteri,[28] I. M. Peruzzi,[28,*]
M. Piccolo,[28] M. Rama,[28] A. Zallo,[28] A. Buzzo,[29] R. Contri,[29] M. Lo Vetere,[29] M. M. Macri,[29] M. R. Monge,[29]
S. Passaggio,[29] C. Patrignani,[29] E. Robutti,[29] A. Santroni,[29] S. Tosi,[29] G. Brandenburg,[30] K. S. Chaisanguanthum,[30]
M. Morii,[30] J. Wu,[30] R. S. Dubitzky,[31] J. Marks,[31] S. Schenk,[31] U. Uwer,[31] D. J. Bard,[32] W. Bhimji,[32] D. A. Bowerman,[32]
P. D. Dauncey,[32] U. Egede,[32] R. L. Flack,[32] J. A. Nash,[32] M. B. Nikolich,[32] W. Panduro Vazquez,[32] P. K. Behera,[33]
X. Chai,[33] M. J. Charles,[33] U. Mallik,[33] N. T. Meyer,[33] V. Ziegler,[33] J. Cochran,[34] H. B. Crawley,[34] L. Dong,[34] V. Eyges,[34]
W. T. Meyer,[34] S. Prell,[34] E. I. Rosenberg,[34] A. E. Rubin,[34] A. V. Gritsan,[35] A. G. Denig,[36] M. Fritsch,[36] G. Schott,[36]
N. Arnaud,[37] M. Davier,[37] G. Grosdidier,[37] A. Höcker,[37] F. Le Diberder,[37] V. Lepeltier,[37] A. M. Lutz,[37] A. Oyanguren,[37]
S. Pruvot,[37] S. Rodier,[37] P. Roudeau,[37] M. H. Schune,[37] A. Stocchi,[37] W. F. Wang,[37] G. Wormser,[37] C. H. Cheng,[38]
D. J. Lange,[38] D. M. Wright,[38] C. A. Chavez,[39] I. J. Forster,[39] J. R. Fry,[39] E. Gabathuler,[39] R. Gamet,[39] K. A. George,[39]
D. E. Hutchcroft,[39] D. J. Payne,[39] K. C. Schofield,[39] C. Touramanis,[39] A. J. Bevan,[40] F. Di Lodovico,[40] W. Menges,[40]
R. Sacco,[40] G. Cowan,[41] H. U. Flaecher,[41] D. A. Hopkins,[41] P. S. Jackson,[41] T. R. McMahon,[41] S. Ricciardi,[41]
F. Salvatore,[41] A. C. Wren,[41] D. N. Brown,[42] C. L. Davis,[42] J. Allison,[43] N. R. Barlow,[43] R. J. Barlow,[43] Y. M. Chia,[43]
C. L. Edgar,[43] G. D. Lafferty,[43] M. T. Naisbit,[43] J. C. Williams,[43] J. I. Yi,[43] C. Chen,[44] W. D. Hulsbergen,[44] A. Jawahery,[44]
C. K. Lae,[44] D. A. Roberts,[44] G. Simi,[44] G. Blaylock,[45] C. Dallapiccola,[45] S. S. Hertzbach,[45] X. Li,[45] T. B. Moore,[45]
S. Saremi,[45] H. Staengle,[45] R. Cowan,[46] G. Sciolla,[46] S. J. Sekula,[46] M. Spitznagel,[46] F. Taylor,[46] R. K. Yamamoto,[46]
H. Kim,[47] S. E. Mclachlin,[47] P. M. Patel,[47] S. H. Robertson,[47] A. Lazzaro,[48] V. Lombardo,[48] F. Palombo,[48] J. M. Bauer,[49]
L. Cremaldi,[49] V. Eschenburg,[49] R. Godang,[49] R. Kroeger,[49] D. A. Sanders,[49] D. J. Summers,[49] H. W. Zhao,[49] S. Brunet,[50]
D. Côté,[50] M. Simard,[50] P. Taras,[50] F. B. Viaud,[50] H. Nicholson,[51] N. Cavallo,[52,†] G. De Nardo,[52] F. Fabozzi,[52,†] C. Gatto,[52]
L. Lista,[52] D. Monorchio,[52] P. Paolucci,[52] D. Piccolo,[52] C. Sciacca,[52] M. A. Baak,[53] G. Raven,[53] H. L. Snoek,[53]
C. P. Jessop,[54] J. M. LoSecco,[54] T. Allmendinger,[55] G. Benelli,[55] L. A. Corwin,[55] K. K. Gan,[55] K. Honscheid,[55]
D. Hufnagel,[55] P. D. Jackson,[55] H. Kagan,[55] R. Kass,[55] A. M. Rahimi,[55] J. J. Regensburger,[55] R. Ter-Antonyan,[55]
Q. K. Wong,[55] N. L. Blount,[56] J. Brau,[56] R. Frey,[56] O. Igonkina,[56] J. A. Kolb,[56] M. Lu,[56] R. Rahmat,[56] N. B. Sinev,[56]

PHYSICAL REVIEW LETTERS

D. Strom,[56] J. Strube,[56] E. Torrence,[56] A. Gaz,[57] M. Margoni,[57] M. Morandin,[57] A. Pompili,[57] M. Posocco,[57]
M. Rotondo,[57] F. Simonetto,[57] R. Stroili,[57] C. Voci,[57] M. Benayoun,[58] H. Briand,[58] J. Chauveau,[58] P. David,[58]
L. Del Buono,[58] Ch. de la Vaissière,[58] O. Hamon,[58] B. L. Hartfiel,[58] Ph. Leruste,[58] J. Malclès,[58] J. Ocariz,[58] L. Roos,[58]
G. Therin,[58] L. Gladney,[59] M. Biasini,[60] R. Covarelli,[60] C. Angelini,[61] G. Batignani,[61] S. Bettarini,[61] F. Bucci,[61]
G. Calderini,[61] M. Carpinelli,[61] R. Cenci,[61] F. Forti,[61] M. A. Giorgi,[61] A. Lusiani,[61] G. Marchiori,[61] M. A. Mazur,[61]
M. Morganti,[61] N. Neri,[61] E. Paoloni,[61] G. Rizzo,[61] J. J. Walsh,[61] M. Haire,[62] D. Judd,[62] D. E. Wagoner,[62] J. Biesiada,[63]
N. Danielson,[63] P. Elmer,[63] Y. P. Lau,[63] C. Lu,[63] J. Olsen,[63] A. J. S. Smith,[63] A. V. Telnov,[63] F. Bellini,[64] G. Cavoto,[64]
A. D'Orazio,[64] D. del Re,[64] E. Di Marco,[64] R. Faccini,[64] F. Ferrarotto,[64] F. Ferroni,[64] M. Gaspero,[64] L. Li Gioi,[64]
M. A. Mazzoni,[64] S. Morganti,[64] G. Piredda,[64] F. Polci,[64] F. Safai Tehrani,[64] C. Voena,[64] M. Ebert,[65] H. Schröder,[65]
R. Waldi,[65] T. Adye,[66] N. De Groot,[66] B. Franek,[66] E. O. Olaiya,[66] F. F. Wilson,[66] R. Aleksan,[67] S. Emery,[67] A. Gaidot,[67]
S. F. Ganzhur,[67] G. Hamel de Monchenault,[67] W. Kozanecki,[67] M. Legendre,[67] G. Vasseur,[67] Ch. Yèche,[67] M. Zito,[67]
X. R. Chen,[68] H. Liu,[68] W. Park,[68] M. V. Purohit,[68] J. R. Wilson,[68] M. T. Allen,[69] D. Aston,[69] R. Bartoldus,[69] P. Bechtle,[69]
N. Berger,[69] R. Claus,[69] J. P. Coleman,[69] M. R. Convery,[69] M. Cristinziani,[69] J. C. Dingfelder,[69] J. Dorfan,[69]
G. P. Dubois-Felsmann,[69] D. Dujmic,[69] W. Dunwoodie,[69] R. C. Field,[69] T. Glanzman,[69] S. J. Gowdy,[69] M. T. Graham,[69]
P. Grenier,[69] V. Halyo,[69] C. Hast,[69] T. Hryn'ova,[69] W. R. Innes,[69] M. H. Kelsey,[69] P. Kim,[69] D. W. G. S. Leith,[69] S. Li,[69]
S. Luitz,[69] V. Luth,[69] H. L. Lynch,[69] D. B. MacFarlane,[69] H. Marsiske,[69] R. Messner,[69] D. R. Muller,[69] C. P. O'Grady,[69]
V. E. Ozcan,[69] A. Perazzo,[69] M. Perl,[69] T. Pulliam,[69] B. N. Ratcliff,[69] A. Roodman,[69] A. A. Salnikov,[69] R. H. Schindler,[69]
J. Schwiening,[69] A. Snyder,[69] J. Stelzer,[69] D. Su,[69] M. K. Sullivan,[69] K. Suzuki,[69] S. K. Swain,[69] J. M. Thompson,[69]
J. Va'vra,[69] N. van Bakel,[69] M. Weaver,[69] A. J. R. Weinstein,[69] W. J. Wisniewski,[69] M. Wittgen,[69] D. H. Wright,[69]
A. K. Yarritu,[69] K. Yi,[69] C. C. Young,[69] P. R. Burchat,[70] A. J. Edwards,[70] S. A. Majewski,[70] B. A. Petersen,[70] C. Roat,[70]
L. Wilden,[70] S. Ahmed,[71] M. S. Alam,[71] R. Bula,[71] J. A. Ernst,[71] V. Jain,[71] B. Pan,[71] M. A. Saeed,[71] F. R. Wappler,[71]
S. B. Zain,[71] W. Bugg,[72] M. Krishnamurthy,[72] S. M. Spanier,[72] R. Eckmann,[73] J. L. Ritchie,[73] A. Satpathy,[73]
C. J. Schilling,[73] R. F. Schwitters,[73] J. M. Izen,[74] X. C. Lou,[74] S. Ye,[74] F. Bianchi,[75] F. Gallo,[75] D. Gamba,[75] M. Bomben,[76]
L. Bosisio,[76] C. Cartaro,[76] F. Cossutti,[76] G. Della Ricca,[76] S. Dittongo,[76] L. Lanceri,[76] L. Vitale,[76] V. Azzolini,[77]
N. Lopez-March,[77] F. Martinez-Vidal,[77] Sw. Banerjee,[78] B. Bhuyan,[78] C. M. Brown,[78] D. Fortin,[78] K. Hamano,[78]
R. Kowalewski,[78] I. M. Nugent,[78] J. M. Roney,[78] R. J. Sobie,[78] J. J. Back,[79] P. F. Harrison,[79] T. E. Latham,[79]
G. B. Mohanty,[79] M. Pappagallo,[79] H. R. Band,[80] X. Chen,[80] B. Cheng,[80] S. Dasu,[80] M. Datta,[80] K. T. Flood,[80]
J. J. Hollar,[80] P. E. Kutter,[80] B. Mellado,[80] A. Mihalyi,[80] Y. Pan,[80] M. Pierini,[80] R. Prepost,[80] S. L. Wu,[80]
Z. Yu,[80] and H. Neal[81]

(*BABAR* Collaboration)

[1]*Laboratoire de Physique des Particules, IN2P3/CNRS et Université de Savoie, F-74941 Annecy-Le-Vieux, France*
[2]*Universitat de Barcelona, Facultat de Fisica, Departament ECM, E-08028 Barcelona, Spain*
[3]*Università di Bari, Dipartimento di Fisica and INFN, I-70126 Bari, Italy*
[4]*Institute of High Energy Physics, Beijing 100039, China*
[5]*University of Bergen, Institute of Physics, N-5007 Bergen, Norway*
[6]*Lawrence Berkeley National Laboratory and University of California, Berkeley, California 94720, USA*
[7]*University of Birmingham, Birmingham, B15 2TT, United Kingdom*
[8]*Ruhr Universität Bochum, Institut für Experimentalphysik 1, D-44780 Bochum, Germany*
[9]*University of Bristol, Bristol BS8 1TL, United Kingdom*
[10]*University of British Columbia, Vancouver, British Columbia, Canada V6T 1Z1*
[11]*Brunel University, Uxbridge, Middlesex UB8 3PH, United Kingdom*
[12]*Budker Institute of Nuclear Physics, Novosibirsk 630090, Russia*
[13]*University of California at Irvine, Irvine, California 92697, USA*
[14]*University of California at Los Angeles, Los Angeles, California 90024, USA*
[15]*University of California at Riverside, Riverside, California 92521, USA*
[16]*University of California at San Diego, La Jolla, California 92093, USA*
[17]*University of California at Santa Barbara, Santa Barbara, California 93106, USA*
[18]*University of California at Santa Cruz, Institute for Particle Physics, Santa Cruz, California 95064, USA*
[19]*California Institute of Technology, Pasadena, California 91125, USA*
[20]*University of Cincinnati, Cincinnati, Ohio 45221, USA*
[21]*University of Colorado, Boulder, Colorado 80309, USA*
[22]*Colorado State University, Fort Collins, Colorado 80523, USA*
[23]*Universität Dortmund, Institut für Physik, D-44221 Dortmund, Germany*

[24]Technische Universität Dresden, Institut für Kern- und Teilchenphysik, D-01062 Dresden, Germany

[25]Laboratoire Leprince-Ringuet, CNRS/IN2P3, Ecole Polytechnique, F-91128 Palaiseau, France

[26]University of Edinburgh, Edinburgh EH9 3JZ, United Kingdom

[27]Università di Ferrara, Dipartimento di Fisica and INFN, I-44100 Ferrara, Italy

[28]Laboratori Nazionali di Frascati dell'INFN, I-00044 Frascati, Italy

[29]Università di Genova, Dipartimento di Fisica and INFN, I-16146 Genova, Italy

[30]Harvard University, Cambridge, Massachusetts 02138, USA

[31]Universität Heidelberg, Physikalisches Institut, Philosophenweg 12, D-69120 Heidelberg, Germany

[32]Imperial College London, London, SW7 2AZ, United Kingdom

[33]University of Iowa, Iowa City, Iowa 52242, USA

[34]Iowa State University, Ames, Iowa 50011-3160, USA

[35]Johns Hopkins University, Baltimore, Maryland 21218, USA

[36]Universität Karlsruhe, Institut für Experimentelle Kernphysik, D-76021 Karlsruhe, Germany

[37]Laboratoire de l'Accélérateur Linéaire, IN2P3/CNRS et Université Paris-Sud 11, Centre Scientifique d'Orsay,
B.P. 34, F-91898 ORSAY Cedex, France

[38]Lawrence Livermore National Laboratory, Livermore, California 94550, USA

[39]University of Liverpool, Liverpool L69 7ZE, United Kingdom

[40]Queen Mary, University of London, E1 4NS, United Kingdom

[41]University of London, Royal Holloway and Bedford New College, Egham, Surrey TW20 0EX, United Kingdom

[42]University of Louisville, Louisville, Kentucky 40292, USA

[43]University of Manchester, Manchester M13 9PL, United Kingdom

[44]University of Maryland, College Park, Maryland 20742, USA

[45]University of Massachusetts, Amherst, Massachusetts 01003, USA

[46]Massachusetts Institute of Technology, Laboratory for Nuclear Science, Cambridge, Massachusetts 02139, USA

[47]McGill University, Montréal, Québec, Canada H3A 2T8

[48]Università di Milano, Dipartimento di Fisica and INFN, I-20133 Milano, Italy

[49]University of Mississippi, University, Mississippi 38677, USA

[50]Université de Montréal, Physique des Particules, Montréal, Québec, Canada H3C 3J7

[51]Mount Holyoke College, South Hadley, Massachusetts 01075, USA

[52]Università di Napoli Federico II, Dipartimento di Scienze Fisiche and INFN, I-80126, Napoli, Italy

[53]NIKHEF, National Institute for Nuclear Physics and High Energy Physics, NL-1009 DB Amsterdam, The Netherlands

[54]University of Notre Dame, Notre Dame, Indiana 46556, USA

[55]The Ohio State University, Columbus, Ohio 43210, USA

[56]University of Oregon, Eugene, Oregon 97403, USA

[57]Università di Padova, Dipartimento di Fisica and INFN, I-35131 Padova, Italy

[58]Laboratoire de Physique Nucléaire et de Hautes Energies, IN2P3/CNRS, Université Pierre et Marie Curie-Paris 6,
Université Denis Diderot-Paris 7, F-75252 Paris, France

[59]University of Pennsylvania, Philadelphia, Pennsylvania 19104, USA

[60]Università di Perugia, Dipartimento di Fisica and INFN, I-06100 Perugia, Italy

[61]Università di Pisa, Dipartimento di Fisica, Scuola Normale Superiore and INFN, I-56127 Pisa, Italy

[62]Prairie View A&M University, Prairie View, Texas 77446, USA

[63]Princeton University, Princeton, New Jersey 08544, USA

[64]Università di Roma La Sapienza, Dipartimento di Fisica and INFN, I-00185 Roma, Italy

[65]Universität Rostock, D-18051 Rostock, Germany

[66]Rutherford Appleton Laboratory, Chilton, Didcot, Oxon, OX11 0QX, United Kingdom

[67]DSM/Dapnia, CEA/Saclay, F-91191 Gif-sur-Yvette, France

[68]University of South Carolina, Columbia, South Carolina 29208, USA

[69]Stanford Linear Accelerator Center, Stanford, California 94309, USA

[70]Stanford University, Stanford, California 94305-4060, USA

[71]State University of New York, Albany, New York 12222, USA

[72]University of Tennessee, Knoxville, Tennessee 37996, USA

[73]University of Texas at Austin, Austin, Texas 78712, USA

[74]University of Texas at Dallas, Richardson, Texas 75083, USA

[75]Università di Torino, Dipartimento di Fisica Sperimentale and INFN, I-10125 Torino, Italy

[76]Università di Trieste, Dipartimento di Fisica and INFN, I-34127 Trieste, Italy

[77]IFIC, Universitat de Valencia-CSIC, E-46071 Valencia, Spain

[78]University of Victoria, Victoria, British Columbia, Canada V8W 3P6

[79]Department of Physics, University of Warwick, Coventry CV4 7AL, United Kingdom

[80]University of Wisconsin, Madison, Wisconsin 53706, USA

[81]Yale University, New Haven, Connecticut 06511, USA

We measure the branching fraction ($\mathcal{B}$), polarization (f_L), and *CP* asymmetry (A_{CP}) of $B^\pm \to \rho^\pm\rho^0$ decays and search for the decay $B^\pm \to \rho^\pm f_0(980)$ based on a data sample of 231.8×10^6 $\Upsilon(4S) \to B\bar{B}$ decays collected with the *BABAR* detector at the SLAC PEP-II asymmetric-energy *B* factory. In $B^\pm \to \rho^\pm\rho^0$ decays we measure $\mathcal{B} = (16.8 \pm 2.2 \pm 2.3) \times 10^{-6}$, $f_L = 0.905 \pm 0.042^{+0.023}_{-0.027}$, and $A_{CP} = -0.12 \pm 0.13 \pm 0.10$, and find an upper limit on the branching fraction of $B^\pm \to \rho^\pm f_0(980)(\to \pi^+\pi^-)$ decays of 1.9×10^{-6} at 90% confidence level.

The measurement of the *CP*-violating phase of the Cabibbo-Kobayashi-Maskawa (CKM) quark-mixing matrix [1] is an important part of the present program in particle physics. Violation of *CP* symmetry is manifested as a nonzero area of the CKM unitarity triangle [2]. In this Letter we report the measurement of the branching fraction, polarization, and *CP* asymmetry of the $B^\pm \to \rho^\pm\rho^0$ decay mode, which is needed for the $\rho\rho$ isospin analysis used to extract $\alpha = \arg[-V_{td}V_{tb}^*/V_{ud}V_{ub}^*]$ [3]. We also set an upper limit on the unknown branching fraction of $B^\pm \to \rho^\pm f_0(980)(\to \pi^+\pi^-)$, which is measured to control this background to the $B^\pm \to \rho^\pm\rho^0$ analysis.

In $B^0(\bar{B}^0) \to \rho^+\rho^-$ decays [4] the interference between the $B\bar{B}$ oscillations which depend on V_{td} and the dominating tree-level amplitude $b \to u\bar{u}d$ causes a time-dependent *CP* asymmetry that depends on $\sin(2\alpha)$. The presence of loop (penguin) amplitudes leads to a shift $\delta\alpha = |\alpha - \alpha_{\text{eff}}^{\rho\rho}|$, between the physical weak phase α and the effective one $\alpha_{\text{eff}}^{\rho\rho}$, experimentally measured in $B^0 \to \rho^+\rho^-$ decays [5,6]. However, the penguin amplitudes in these decays are known to contribute at a very low level because of the small upper limit of 1.1×10^{-6} at 90%

confidence level (C.L.) [7], obtained from the branching fraction of the penguin dominated mode $B^0 \to \rho^0\rho^0$. The size of $\delta\alpha$ can be extracted from the full isospin analysis combining all $B \to \rho\rho$ modes [3].

In $B \to \rho\rho$ decays, a spin zero particle decays into two spin one particles. The final state is therefore a superposition of two transversely polarized modes (helicity ± 1) and one longitudinal mode (helicity 0), which can be measured through an angular analysis. The longitudinal polarization fraction f_L is defined as the fraction of decays to the helicity zero state $f_L = \Gamma_L/\Gamma$, where Γ is the total decay rate and Γ_L is the decay rate to the longitudinally polarized final state. The transverse polarization is a mixed *CP* state, while the longitudinal state is pure *CP* even. The previous measurements of f_L [8,9] showed the decay is consistent with being fully longitudinally polarized.

Our analysis is performed in the helicity frame [10] as a function of the two helicity angles $\theta_\pm$ and θ_0 where the helicity angle of a $\rho^\pm(\rho^0)$ meson is defined as the angle between its daughter $\pi^\pm(\pi^+)$ and the direction opposite to the *B* meson in the $\rho^\pm$ (ρ^0) rest frame. The polarization f_L can be extracted from the differential decay rate:

$$\frac{1}{\Gamma}\frac{d^2\Gamma}{d\cos\theta_\pm\,d\cos\theta_0} = \frac{9}{4}\left[f_L\cos^2\theta_\pm\cos^2\theta_0 + \frac{1}{4}(1-f_L)\sin^2\theta_\pm\sin^2\theta_0\right].$$ (1)

Here we integrate over the angle between the ρ-meson decay planes.

The measurements presented in this Letter are based on data collected with the *BABAR* detector [11] at the SLAC PEP-II asymmetric-energy e^+e^- collider. The analyzed data sample of $(231.8 \pm 2.6) \times 10^6$ $B\bar{B}$ pairs produced at the $\Upsilon(4S)$ resonance corresponds to an integrated luminosity of 210.5 fb^{-1}.

To reconstruct $B^\pm \to \rho^\pm\rho^0$ and $B^\pm \to \rho^\pm f_0$ decays, we select events with at least three charged tracks and one neutral pion candidate. Charged tracks are required to originate from the interaction point and have particle identification information inconsistent with kaon, electron, and proton hypotheses. We form $\pi^0 \to \gamma\gamma$ candidates from pairs of calorimeter showers, each with a photonlike lateral spread and a minimum energy of 50 MeV. The invariant mass of π^0 candidates is required to fall in the range $0.10 < m_{\gamma\gamma} < 0.16$ GeV/c^2.

The mass of charged $\rho^\pm$ candidates must satisfy $0.396 < m_{\pi^\pm\pi^0} < 1.146$ GeV/c^2 where the lowside re-

quirement on the $\pi^\pm\pi^0$ mass is chosen to exclude $K_S^0 \to \pi^+\pi^-$ decays. Neutral final state meson candidates (ρ^0, f_0) must satisfy $0.520 < m_{\pi^+\pi^-} < 1.146$ GeV/c^2. In order to suppress backgrounds with low momentum pions, the helicity angles are required to fall in the ranges $-0.8 < \cos\theta_\pm < 0.95$ and $|\cos\theta_0| < 0.95$. Backgrounds from $D^0 \to K^-\pi^+\pi^0$ and $D^0 \to \pi^-\pi^+\pi^0$ decays are reduced by requiring the candidate D^0 invariant mass to be at least 40 MeV/c^2 away from the D^0 mass.

About 20% of the selected events have multiple *B* candidates and the one that has the reconstructed π^0 mass closest to the π^0 mass is kept. In the case that more than one candidate has the same reconstructed π^0 mass, we select one at random.

Continuum decays represent the largest source of background and are reduced by requiring $|\cos\theta_T| < 0.8$, where θ_T is the cosine of the angle between the *B* thrust axis and that from the rest of the event (ROE). To further discriminate signal from continuum, we also use a neural network built out of five event-shape variables: a Fisher discrimi-

nant combining the 0th and 2nd order monomials [12] for charged particles and neutral clusters of the ROE; the cosine of the angle between the direction of the B and the collision axis (z) in the center-of-mass (c.m.) frame; the cosine of the angle between the B thrust axis and the z axis; the variable $|\cos\theta_T|$ defined above; and the sum of transverse momenta in the ROE relative to the z axis. The output is transformed into a variable x_{NN} which has roughly Gaussian signal and background distributions. We select candidates in a range of x_{NN} that removes 54% of continuum background events while retaining 90% of the signal. After these selections, about 85% of the remaining events are from continuum decays.

Signal event candidates are further identified based on two kinematic variables: the beam-energy-substituted mass $m_{ES} = \sqrt{(s/2 + \mathbf{p}_i \cdot \mathbf{p}_B)^2/E_i^2 - \mathbf{p}_B^2}$, using the total initial e^+e^- 4-momentum (E_i, $\mathbf{p}_i$), c.m. energy ($\sqrt{s}$) and the B momentum ($\mathbf{p}_B$), and $\Delta E = E_B^* - \sqrt{s}/2$, the difference between the reconstructed B energy in the c.m. frame (E_B^*) and the beam energy. Events are selected if $m_{ES} >$ 5.26 GeV/c^2 and $|\Delta E| <$ 150 MeV.

After the selection criteria are applied, the efficiency is 8.4% for longitudinal and 18.6% for transverse polarized $B^\pm \rightarrow \rho^\pm \rho^0$ decays. The selection efficiency is 16.6% for $B^\pm \rightarrow \rho^\pm f_0$ decays. Any possible interference effects between the $B^\pm \rightarrow \rho^\pm \rho^0$ and $B^\pm \rightarrow \rho^\pm f_0$ are neglected.

An unbinned extended maximum likelihood fit is applied to the selected sample of $N_{tot} = 74293$ events in order to measure the $B^\pm \rightarrow \rho^\pm \rho^0$ event yield, polarization, and charge asymmetry as well as the $B^\pm \rightarrow \rho^\pm f_0$ event yield. The likelihood function is

$$\mathcal{L} = \frac{1}{N_{tot}!} \exp\left(-\sum_{k=1}^{M} n_k\right) \prod_{i=1}^{N_{tot}} \left[\sum_{j=1}^{M} n_j \mathcal{P}_j(\vec{x}_i)\right], \quad (2)$$

where M is the number of hypotheses (signal, misreconstructed signal, continuum, and B-background classes), and n_k (n_j) represents the number of measured events for each hypothesis determined by maximizing the likelihood function. $\mathcal{P}_j(\vec{x}_i)$ is the product of the probability density functions (PDFs) of hypothesis j evaluated at the ith event's measured variables, $\vec{x}_i = \{m_{ES}, \Delta E, m_{\pi^\pm\pi^0}, m_{\pi^+\pi^-}, \cos\theta_\pm, \cos\theta_0, x_{NN}\}$. In addition, the charge asymmetry, obtained from the measured B^- and B^+ signal candidate decay yields, $A_{CP} = \frac{N_{B^-}-N_{B^+}}{N_{B^-}+N_{B^+}}$, is determined in the fit to the data.

Each discriminating variable in the likelihood function is modeled with a PDF extracted either from the data, or from high statistics Monte Carlo (MC) simulated data samples. The correlations between the variables are assumed to be small and the PDFs independent. This is checked with systematic error studies, and corrections are applied where necessary.

The continuum background ΔE, m_{ES}, and x_{NN} distributions are modeled with one-dimensional parametrized distributions taken from fits to the data. Correlations are observed between the $m_{\pi\pi}$ and $\cos\theta$ distributions for both ρ-meson candidates, which are taken into account with two-dimensional PDFs. The signal component is modeled with one-dimensional parametrized distributions for each of six variables; m_{ES} is modeled with a nonparametric PDF [13]. The signal PDF shapes are obtained from fits to signal MC sample after the selection is applied. Events with a true $B^\pm \rightarrow \rho^\pm \rho^0$ decay but with wrong tracks or calorimeter clusters assigned to the final state are referred to as self cross feed (SCF) events. They make up 35% and 14% of the selected longitudinally and transversely polarized signal samples, respectively. The longitudinal and transverse SCF components and B-background PDFs are determined in a similar manner using high statistics MC samples and modeled with nonparametric PDFs [13] for each variable.

To understand the backgrounds from other B decay modes we use MC simulated events. There are two types of B background: "charmed" (decays involving $b \rightarrow c$ transitions), and "charmless" (all other b decays). Altogether 16 B-background categories plus the two SCF components are included in the fit. The SCF yields and polarization are fixed in the final fit at values that match those fitted for the signal in previous iterations of the fit. Four specific charmed background modes are included: $B^- \rightarrow D^0\pi^-$, $B^- \rightarrow D^0\rho^-$, $B^- \rightarrow D^{*0}\pi^-$, and $B^- \rightarrow D^{*0}\rho^-$. Other charmed backgrounds are combined into two generic classes of events for charged and neutral charmed B decays. For the charmless B backgrounds, separate MC samples of eight modes were used: neutral B decaying to $\rho^+\rho^-$ and charged B decaying to $\rho^\pm f_0(980)$, $\eta'\rho^\pm$, $K^{*0}\rho^\pm$, $a_1^0\pi^\pm$, $a_1^\pm\pi^0$, $a_1^\pm\rho^0$, and $a_1^0\rho^\pm$ with the decays $a_1^0 \rightarrow (\rho\pi)^0$ and $a_1^\pm \rightarrow (\rho\pi)^\pm$. For B decaying to vector mesons, only the longitudinal component of the decay is considered. Two generic categories, one for 5-body modes and one for all "other charmless" decays, complete the B-background model.

The number of "other charmless" events and the $B^\pm \rightarrow \rho^\pm f_0$ yield were determined from the data fit. The other 14 backgrounds had their yields fixed in the fit. We use the following branching fractions: $\mathcal{B}(B^0 \rightarrow \rho^+\rho^-) = (26.2 \pm 3.7) \times 10^{-6}$ [14], $\mathcal{B}(B^\pm \rightarrow \eta'\rho^\pm) = (12.9 \pm 6.5) \times 10^{-6}$ [15], $\mathcal{B}(\eta' \rightarrow \rho^0\gamma) = 0.295 \pm 0.010$ [16], $\mathcal{B}(B^+ \rightarrow K^{*0}\rho^+) = (10.5 \pm 1.8) \times 10^{-6}$ [14], and $\mathcal{B}(K^{*0} \rightarrow K^+\pi^-) = 2/3$. The decays $B^\pm \rightarrow (a_1\pi)^\pm$ and $B^\pm \rightarrow (a_1\rho)^\pm$ have few experimental constraints [17,18]. We adopt the following $B^\pm$ branching ratios, in units of 10^{-6}, and assume a 100% systematic uncertainty: $a_1^0\pi^+ = 12$, $a_1^+\pi^0 = 6$, $a_1^0\rho^+ = a_1^+\rho^0 = 48$.

Table I shows the results of the fit, where the quoted errors are statistical errors only. Projection plots for m_{ES} and ΔE are shown in Fig. 1.

TABLE I. Summary of the results of the fit with statistical errors (before correction for fit biases).

Observables	Fitted value
$B^\pm \to \rho^\pm \rho^0$ yield	390 ± 49 events
Polarization f_L	0.897 ± 0.042
Charge asymmetry A_{CP}	-0.12 ± 0.13
$B^\pm \to \rho^\pm f_0$ yield	51 ± 30 events

TABLE II. Summary of the systematic uncertainties on the $B^\pm \to \rho^\pm \rho^0$ yield, the polarization f_L, and the $B^\pm \to \rho^\pm f_0$ yield.

Source	$\rho^\pm \rho^0$ yield	f_L	$\rho^\pm f_0$ yield
Fit bias uncertainty	27.3	0.005	9.8
B-background rates	11.0	0.007	2.8
Nonresonant backgrounds	12.0	0.009	3.0
Amount of SCF	24.0	0.010	0.6
PDF shapes	$+21.1$ -22.5	$+0.017$ -0.022	$+7.9$ -13.5
f_0 mass and width	$+0.9$ -0.6	0.000	3.9
Total	$+45$ -46	$+0.023$ -0.027	$+14$ -18

We considered systematic effects from biases in the fit model, which are due to the imperfect modeling of some correlations between fitted variables in the likelihood function. Tests of the fit are made by using a large number of MC samples containing the amounts of signal, continuum, and B-background events measured or fixed in the data fit, and where correlations between variables are modeled for signal and B backgrounds. The fits to these samples should reproduce the number of MC events generated. A shift of the fitted values with respect to the generated ones indicates a bias of -49 events on the $\rho^\pm \rho^0$ yield, $+0.009$ on f_L, and -4.6 events on the $\rho^\pm f_0$ yield in the fitting procedure. We use the same technique to study the effects of correlations between the neural net and helicity variables in the $q\bar{q}$ continuum and observe a fit bias of $+24$ events on the $\rho^\pm \rho^0$ yield, -0.001 on f_L, and -19 events on the $\rho^\pm f_0$ yield. No other significant correlations were observed between the other discriminating variables. These two biases are corrected from the fit measurements, and half of each separate fit bias is taken as the systematic error (cf. Table II).

Many of the B-background rates are poorly known. The effect of uncertainties in these values is evaluated by varying the number of events in each background category within the range allowed by the error on the branching fraction. Fourteen nonresonant backgrounds that are not in the default fit are tested by adding them singly to the fit with a yield that is allowed to vary. The only shift seen was associated with the mode $B^\pm \to \pi^\pm \pi^0 \pi^0$, and is taken as a symmetric systematic uncertainty.

The systematic error associated with misreconstructed signal is evaluated by taking the difference between the default fit and the one for which these events are not modeled, and therefore mostly absorbed into the "other charmless" background category. We consider the error due to the uncertainty on the signal, B background, and continuum PDF shapes and estimate a systematic error by varying the parameters obtained from MC calculations that govern these shapes within their statistical uncertainty. The impact of the uncertainty on the measurement of the f_0 mass and width [19] has also been evaluated. The values of the systematic errors described above are given in Table II.

Systematic uncertainties in the reconstruction and calibration procedure introduce a systematic error of 3% after a correction of -2.5% on the π^0 reconstruction efficiency, 3.9% after a correction of -1.5% on the track reconstruction efficiency, and a systematic error of 1.1% from the particle identification. The uncertainty on the efficiency ratio between longitudinal and transverse events is found to be negligible. The error on A_{CP} includes a 0.45% uncertainty in the charged track reconstruction asymmetry, a 4% uncertainty from the detector's intrinsic charged particle identification asymmetry, and a 9% uncertainty which is the largest single shift obtained when assuming a uniform probability for the charge asymmetry of every B-background individually.
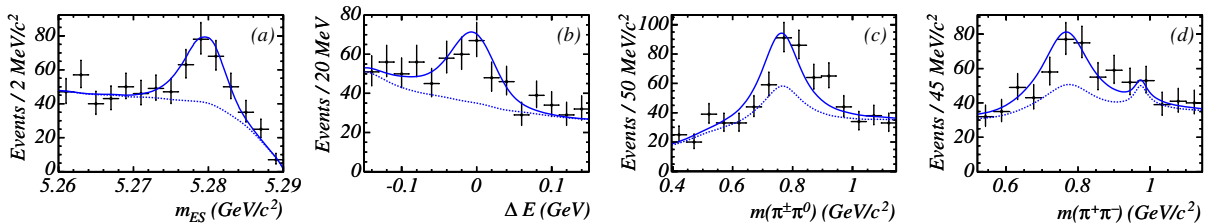

FIG. 1 (color online).   Projections of (a) $m_{\rm ES}$, (b) ΔE, (c) $m_{\pi^\pm \pi^0}$, and (d) $m_{\pi^+ \pi^-}$ with a cut on the ratio of the signal and background likelihoods that selects about 40% of the signal. For (a) and (b), the observable plotted is excluded from the fit in calculating the likelihood used for the enrichment selection. For (c) and (d), only the $m_{\rm ES}$, ΔE, and x_{NN} variables have been used in calculating the likelihood. Points represent on-resonance data, dashed lines the continuum and $B\bar{B}$ backgrounds PDFs, and solid lines the likelihood function with yields taken from the fit where all variables have been used.

In summary, we measure the branching fraction, longitudinal polarization, and *CP* asymmetry of the decay $B^\pm \to \rho^\pm \rho^0$, using a dataset of about 231.8×10^6 $B\bar{B}$ pairs, to be

$$\mathcal{B}(B^\pm \to \rho^\pm \rho^0) = (16.8 \pm 2.2 \pm 2.3) \times 10^{-6},$$

$$f_L(B^\pm \to \rho^\pm \rho^0) = 0.905 \pm 0.042^{+0.023}_{-0.027},$$

$$A_{CP}(B^\pm \to \rho^\pm \rho^0) = -0.12 \pm 0.13 \pm 0.10.$$

The measurement of the branching fraction has improved by a factor of about 2 with respect to the previous *BABAR* measurement [8], and supersedes it. The isospin relations between branching ratios are consistent between this measurement and those of $\rho^+\rho^-$ and $\rho^0\rho^0$ [14], validating the approach [3] used to constraint α. Moreover, our measurements confirm that this mode is largely longitudinally polarized. They also confirm that the charge asymmetry is consistent with zero as expected for decays proceeding through one decay channel only; this suggests the contributions of electroweak penguins are small in the $B \to \rho\rho$ system.

In addition we measure

$$\mathcal{B}(B^\pm \to \rho^\pm f_0(980)(\to \pi^+\pi^-)) = (0.7 \pm 0.8 \pm 0.5) \times 10^{-6}$$

with a significance of 0.4σ. We set an upper limit on the branching fraction of 1.9×10^{-6} at 90% confidence level by finding the yield (N) that satisfies $\int_0^N \mathcal{L}(n)dn / \int_0^\infty \mathcal{L}(n)dn = 0.9$ taking into account systematic uncertainties.

*Also with Università di Perugia, Dipartimento di Fisica, Perugia, Italy

†Also with Università della Basilicata, Potenza, Italy

[1] N. Cabibbo, Phys. Rev. Lett. **10**, 531 (1963); M. Kobayashi and T. Maskawa, Prog. Theor. Phys. **49**, 652 (1973).

[2] C. Jarlskog, Phys. Rev. Lett. **55**, 1039 (1985).

[3] M. Gronau and D. London, Phys. Rev. Lett. **65**, 3381 (1990).

[4] Charge conjugation is implied throughout this document, unless explicitly stated.

[5] B. Aubert *et al.* (*BABAR* Collaboration), Phys. Rev. Lett. **95**, 041805 (2005).

[6] A. Somov *et al.* (Belle Collaboration), Phys. Rev. Lett. **96**, 171801 (2006).

[7] B. Aubert *et al.* (*BABAR* Collaboration), Phys. Rev. Lett. **94**, 131801 (2005).

[8] B. Aubert *et al.* (*BABAR* Collaboration), Phys. Rev. Lett. **91**, 171802 (2003).

[9] J. Zhang *et al.* (Belle Collaboration), Phys. Rev. Lett. **91**, 221801 (2003).

[10] G. Kramer and W. F. Palmer, Phys. Rev. D **45**, 193 (1992).

[11] B. Aubert *et al.* (*BABAR* Collaboration), Nucl. Instrum. Methods Phys. Res., Sect. A **479**, 1 (2002).

[12] B. Aubert *et al.* (*BABAR* Collaboration), Phys. Rev. Lett. **89**, 281802 (2002).

[13] K. S. Cranmer, Comput. Phys. Commun. **136**, 198 (2001).

[14] Heavy Flavor Averaging Group (HFAG), hep-ex/0603003.

[15] B. Aubert *et al.* (*BABAR* Collaboration), Phys. Rev. D **70**, 032006 (2004).

[16] S. Eidelman *et al.*, Phys. Lett. B **592**, 1 (2004).

[17] B. Aubert *et al.* (*BABAR* Collaboration), Phys. Rev. Lett. **97**, 051802 (2006).

[18] B. Aubert *et al.* (*BABAR* Collaboration), Phys. Rev. D **74**, 031104 (2006).

[19] E. M. Aitala *et al.* (E791 Collaboration), Phys. Rev. Lett. **86**, 765 (2001).